Deep-Sea Research I 95 (2015) 75–84

Contents lists available at ScienceDirect

Deep-Sea Research I

journal homepage: www.elsevier.com/locate/dsri

High density of ice krill (*Euphausia crystallorophias*) in the Amundsen sea coastal polynya, Antarctica

Hyoung Sul La [a], Hyungbeen Lee [b], Sophie Fielding [c], Donhyug Kang [d], Ho Kyung Ha [e], Angus Atkinson [f], Jisoo Park [a], Volker Siegel [g], SangHoon Lee [a], Hyoung Chul Shin [a,*]

[a] Division of Polar Ocean Environment, Korea Polar Research Institute, Korea Institute of Ocean Science and Technology, Incheon 406-840, South Korea
[b] Fisheries System Engineering Division, National Fisheries Research and Development Institute, Korea
[c] British Antarctic Survey, Natural Environment Research Council, Madingley Road, Cambridge CB3 OET, United Kingdom
[d] Maritime Security Research Center, Korea Institute of Ocean Science and Technology, South Korea
[e] Department of Ocean Sciences, Inha University, Incheon, 402-751, South Korea
[f] Plymouth Marine Laboratory, The Hoe, Plymouth, PL1 3DH, United Kingdom
[g] Thuenen Institute of Sea Fisheries, Palmaille 9, Hamburg, 22767, Germany

ARTICLE INFO

Article history:
Received 26 August 2013
Received in revised form
22 July 2014
Accepted 3 September 2014
Available online 16 September 2014

Keywords:
Ice krill (*Euphausia crystallorophias*)
krill identification
Acoustic data
Coastal polynya
Amundsen Sea

ABSTRACT

High densities of ice krill *Euphausia crystallorophias* were observed along six acoustic transects within the Amundsen Sea Coastal Polynya, Antarctica. Two-frequency acoustic backscatter data was examined in the austral summers of January 2011 and February 2012. A dB identification window ($S_{v120-38}$) identified ice krill dominating the acoustic backscatter. The density of ice krill, calculated with the stochastic distorted-wave born approximation model, ranged between 4.5 and 30 g wet mass m^{-2} for each transect (a mean of 16 g wet mass m^{-2} for all transects), these high values are an order of magnitude higher than recorded previously in the Ross Sea Polynya. High densities were detected along the ice shelf and near the boundary between pack ice and coastal polynya, and we postulate that these could be important habitats for ice krill. The high densities observed along the transects make ice krill a potentially important, but poorly known contributor to these high-latitude shelf food webs.
© 2014 Elsevier Ltd. All rights reserved.

1. Introduction

Euphausia crystallorophias (Holt and Tattersall, 1906), commonly called “ice krill”, is the most southerly of the krill species and is a keystone species of the neritic ecosystem in the Southern Ocean (Siegel and Piatkowski, 1990; Hosie and Cochran, 1994; Guglielmo et al., 2009). This species is the most abundant euphausiid in the southern high-latitude coastal zones, where it replaces *Euphausia superba* (Thomas and Green, 1988). Ice krill form an important intermediate linkage between primary producers and coastal top predators. These krill appear to be carnivorous prior to the spring bloom but become ominvorous at the start of the spring bloom (Pakhomov et al., 1998, Kittel and Ligowski, 1980) with O'Brien (1987) reporting animal and algal dietary components in a ratio of ~1:1. Although there is sporadic evidence of ice-algal feeding of *E. superba* on the underside of ice floes (Hamner et al., 1983; Melnikov and Spiridinov, 1996), ice krill have been found to occupy the water mass from 1 to 5 m below the ice, but not observed to feed directly on epontic algae (O'Brien, 1987).

Ice krill often provide the principal food source for many key vertebrates (e.g., fish, penguins, and whales) in the high-latitude Antarctic food web (Hubold, 1985; Bushuev, 1986; Whitehead et al., 1990). To understand the role of ice krill in coastal ecosystems, it is important to determine their overall density, spatial and temporal variability in distribution, and how their populations are controlled by the environmental conditions. In this study, we focus on the Amundsen Sea Coastal Polynya (ASCP), which is known to be one of the most productive regions among the identified coastal polynyas surrounding the Antarctic continent (Arrigo and van Dijken, 2003) and constitute an important habitat for ice krill.

Despite the great abundance and ecological significance of ice krill, few acoustic studies have been conducted in coastal polynyas because of the harsh weather and sea ice conditions that limit access. A few available studies of ice krill using net surveys have reported high concentrations of larval, juvenile, and adult stages over the shelf, with maximum densities in regions with permanent polynyas (Pakhomov and Perissinotto, 1996; Pakhomov et al., 1998; Sala et al., 2002; Guglielmo et al., 2009; Lee et al., 2013). In these

* Correspondence to: 213-3 Songdo-dong, Yeonsu-gu, Incheon 406-840, Korea. Tel.: +82 32 760 5333.
E-mail address: hcshin@kopri.re.kr (H.C. Shin).

http://dx.doi.org/10.1016/j.dsr.2014.09.002
0967-0637/© 2014 Elsevier Ltd. All rights reserved.

studies, ice krill were mostly distributed within the uppermost 250 m of water column (Everson, 1987; Pakhomov et al., 1998; Guglielmo et al., 2009). However, the spatial and temporal variability of ice krill in coastal polynyas remains poorly understood, especially within the ASCP.

Polynyas are strongly controlled by physical processes and exhibit steep temporal and spatial gradients of chemical and biological properties, which vary between individual polynyas. There are also inter-annual variations in persistence, in the times of opening and closing, and in the maximum area of open water (Barber and Massom, 2007). The ASCP is a polynya driven by katabatic winds blowing northward from the continental interior, and surrounded by pack ice and the Dotson and Getz ice shelves located off Marie Byrd Land (Fig. 1). It occurs in an identical location each year (Arrigo et al., 2012) and can be geographically subdivided into the ice shelf, fast ice, and the pack ice boundary (Smith and Barber, 2007). The ASCP is generally restricted to the period from October through March and is defined as a region characterized by the absence of sea ice, i.e., where ice concentrations are lower than 10% (Arrigo et al., 2012). It exhibits substantial spatial and temporal variability in the water column because of the variable Antarctic surface water (AASW) and the intrusion of warm and salty Modified Circumpolar Deep Water (MCDW) through the deep trough of the continental shelves in the Dotson Trough (Wåhlin et al., 2013; Ha et al., 2014).

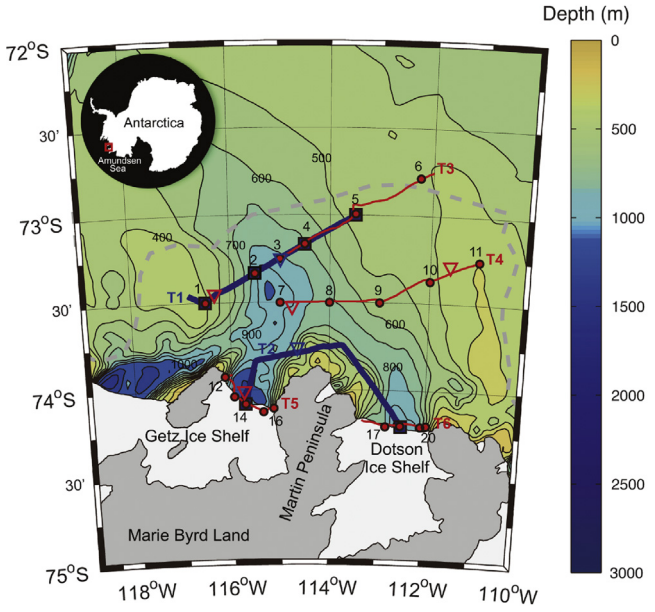

Fig. 1. Study area showing the acoustic transects (blue and red lines for 2011 and 2012, respectively), CTD (blue square for 2011 and red circle for 2012), and net (blue and red reverse triangles for 2011 and 2012, respectively) stations during 2011 and 2012. The dashed gray line indicates the pack ice boundary on the bathymetry of the central Amundsen shelf. (For interpretation of the references to color in this figure legend, the reader is referred to the web version of this article.)

The combination of predictable location and an associated consistently high primary production (Arrigo et al., 2012) make it a natural laboratory to assess the relationship between the ecological characteristics of ice krill and changes in environmental conditions. The aim of this study was to provide the first assessment of distribution and density of ice krill in the ASCP.

2. Materials and methods

2.1. Sampling locations

Acoustic, hydrographic and biological samplings were undertaken in the ASCP during the austral summers of 2011 and 2012 onboard the IBRV *Araon*. Each year, acoustic transects were undertaken within the ASCP. Two transects were completed in 2011—T1 (126 km) in the center of the polynya, and T2 (161 km) from Dotson ice shelf to Getz ice shelf and four transects were completed in 2012—T3 (128 km) and T4 (141 km) in the center of the polynya, and T5 (52 km) at Getz and T6 (46 km) at Dotson (Table 1).

2.2. Environmental data and net sampling

Hydrographic variables were measured at stations along each transect (Fig. 1) using a calibrated conductivity-temperature-depth CTD system (Sea-Bird, SBE 911plus).

The distributions of chlorophyll *a* (Chl *a*) (a proxy for phytoplankton biomass) and sea ice concentrations were estimated from satellite-based data during the survey period. Chl *a* was estimated from 8-day composite Moderate Resolution Imaging Spectroradiometer (MODIS) Aqua Level 3 data (4-km resolution), which was obtained from the Goddard Space Flight Center (McClain et al., 1998). The presence/absence of sea ice at a 6.25-km resolution was estimated from AMSR-E and SSMIS data obtained from the National Snow and Ice Data Center.

Net hauls were conducted along each acoustic transect with a Bongo net (mouth area of 0.5 m^{-2}, 500-μm mesh). Oblique tows from 250 m to the surface were undertaken, and the average towing speed during each haul was 3 knots (range: 2–4 knots). The net hauls were targeted to parameterize the acoustic model used to estimate density using the length-frequency distribution of the sampled krill. A total of six hauls were conducted and each of these averaged 30 to 45 min (Fig. 1). Length measurements (to the nearest mm) were performed from the front of the eye to the tip of the telson (Morris et al., 1988). The length-frequency distributions were estimated based on 300 ice krill individuals each year.

2.3. Acoustic data collection and processing

Volume backscattering data (S_v, dB re 1 m^{-1}) was collected using a Simrad EK60 scientific echosounder system (ER60 software v.2.0.0) configured with 38- and 120-kHz split-beam transducers. The power settings used in 2011 and 2012 were consistent, and the ping rate varied from 2 to 5 s with a pulse length of 1 ms depending on the

Table 1
Details for each acoustic transects surveyed in 2011 and 2012.

Year	Transect	Transect start time (YYYY/MM/DD, GMT)	Transect end time (YYYY/MM/DD, GMT)	Distance (km)	Geographical feature
2011	T1	2011/01/05, 18:10	2011/01/06, 06:36	126	Pack ice boundary
	T2	2011/01/01, 18:08	2011/01/02, 07:00	160	Ice shelf
2012	T3	2012/02/12, 10:37	2012/02/13, 16:02	128	Pack ice boundary
	T4	2012/02/13, 23:33	2012/02/15, 02:15	140	Coastal polynya center
	T5	2012/02/16, 20:48	2012/02/17, 16:33	52	Ice shelf
	T6	2012/02/17, 21:39	2012/02/18, 13:51	43	

Table 2
System parameters of transceiver (Simrad EK60) calibrated for the acoustic surveys in 2011 and 2012.

	2011	2012	
Frequency (kHz)	120	38	120
Transmitted power (W)	500	2000	500
Pulse duration (ms)	1.024	1.024	1.024
Two-way beam angle (dB)	−21.00	−20.60	−21.00
Receiver bandwidth (kHz)	3.03	2.43	3.03
Transducer gain (dB)	25.67	21.35	26.17
3-dB beam angle (along/athwart) (°)	6.67/6.80	7.06/6.99	6.67/6.57
Absorption coefficient (dB km^{-1})	25.94	9.90	24.84
s_A correction	−0.38	−0.44	−0.35
Sound speed (m s^{-1})	1454	1449	1449

synchronization with other acoustic instruments. The nominal vessel speed for data collection on each transect was approximately 6 knots to ensure data quality. The 120-kHz transducer was calibrated following standard procedures (Foote et al., 1987) in the survey region (71°S and 117°W in 2011; 73°S and 117°W in 2012) under calm weather conditions. The 38-kHz transducer was only calibrated in 2012, due to the harsh weather conditions in 2011. The mean temperature through the water column from the transducers to the calibration sphere (approximately 30 m) was −1.6 °C (SD=0.02) in 2011 and −1.7 °C (SD=0.02) in 2012. The 2012 calibration values were applied to the 38 kHz S_v data obtained in both years (Table 2).

The acoustic data was processed using the Myriax Echoview software (v. 4.50). Volume backscattering strength data was collected along the transect periods between stations. Non-biological signals such as surface bubbles, ice fragments, and bottom and false bottom echoes, were identified and excluded. The data was resampled into equivalent distance with dimensions of 5 m (vertical) by 185.2 m (horizontal), and the background noise was removed using the time-varied gain threshold (TVT) function (Myriax, 2012), which was originally conceptualized by Watkins and Brierley (1996). The noise-filtered resampled 38- and 120-kHz echograms were exported from Echoview and imported into Matlab® for further treatment. For analysis the weighted mean depth (WMD) of scattering layer was calculated for each acoustic transect to observe the variability of the main scattering layer in the echogram (Roe et al., 1984).

2.4. Ice krill density estimation

For the density estimates, the 120-kHz S_v attributed to ice krill by the dB window identification was integrated from 10 m below the transducer to 250 m and averaged horizontally to 1852 m (1 nautical mile) to provide a nautical area scattering coefficient (NASC or s_A, m^2nmi^{-2}). A 120–38-kHz two-frequency ($S_{v120-38}$) dB window identification technique combined with a threshold was utilized to identify the ice krill from the acoustic data (Madureira et al., 1993; Demer and Conti, 2005; CCAMLR, 2010). The $S_{v120-38}$ window range was determined using a validated physics-based target strength model, the stochastic distorted-wave born approximation (SDWBA) model (McGehee et al., 1998; Demer and Conti, 2005) and the measured length-frequency of ice krill. The SDWBA was parameterized with length, a density contrast (g) of 1.0357 (Foote, 1990), a sound speed contrast (h) of 1.0279 (Foote, 1990) and a generic body shape (McGehee et al., 1998) fattened by 40% (Conti and Demer, 2006). The SDWBA model was inverted in a least-squares sense to estimate then an in-situ distribution of orientations for the ice krill length frequency distribution obtained during each cruise (Conti and Demer, 2006). The mean and standard deviation of the normal distributions of orientation for the least-squares estimate ranged from −45° to 45° and from 1° to 50°, respectively, in by 1° steps. A mean of 0° indicates krill in a horizontal position and a positive angle represents a head-up position. Because the observed S_v data used in the inversion process was averaged into 185.2-m bins (representing approximately 10 pings) before calculating the mean and standard deviation of the orientation, the calculated standard deviation actually represents the standard error of orientations observed (CCAMLR, 2010). Therefore, the standard error was multiplied by the square root of the number of samples (i.e., $\sqrt{10}$) to estimate the standard deviation. An orientation distribution of N[−8°, 9°] for 2011 and N[13°, 19°] for 2012 was calculated based on $S_{v120-38}$ using a 95% length-frequency distribution. The estimated orientations yield a window of 10.9 to 18.1 dB for 2011 and a window of 12.4 to 17.9 dB for 2012.

The NASC was converted into density estimates (g wet mass m^{-2}) using a weighted conversion factor based on the weight-length relationship used in the CCAMLR synoptic survey (CCAMLR, 2010). The ice krill density was calculated by multiplying the $NASC_{120\ kHz}$ attributed to the ice krill by a factor C, which is equal to the weighted wet weight (W) divided by a weighted spherical scattering cross-section (σ_{sp}) calculated using the SDWBA:

$$\rho = \mathrm{NASC}_{120\ \mathrm{kHz}} C \quad (1)$$

$$C = \Sigma f_i W(L) / \Sigma f_i \sigma_{sp}(L) \quad (2)$$

where ρ is the krill density (g m^{-2}), σ_{sp} is the spherical scattering cross-section (m^2) of individual ice krill as a function of body length (L), W is the ice krill wet mass (g) and f_i is the relative frequency of each length-frequency that sums to 1.

2.5. Statistical analysis

Mann–Whitney U-test was performed to examine the differences of mean S_v and WMD between day and night. We also used the stepwise model selection and generalized linear model (GLM) to predict the spatial variation of ice krill density as a function of environmental variables. This allows for non-linearity and non-normal responses to investigate the combined effects of multiple factors (Hastie and Tibshirani, 1990; Guisan et al., 2002). The hypothesized variables included in the statistical model were: the mean ice krill density (averaged for an area with 1 nmi around each CTD station), the surface potential temperature and salinity (averaged from surface to 20 m), the mean potential temperature and salinity (averaged from surface to top 250 m), the integrated Chl a (surface to 100 m), and water depth at each station during 2011 and 2012. The model selection was based on the Akaike Information Criterion (AIC) with smaller values of AIC being preferred, and a logarithmic link function was assumed (Maunder, et al., 2006).

3. Results

3.1. Hydrographic conditions

The potential temperature (θ)-salinity (S) diagrams indicated the presence of two water masses, namely AASW and MCDW, during 2011 and 2012 (Fig. 2(a) and (b)). The AASW is found in the upper 300 m (in contact with the atmosphere), where it undergoes sensitive and latent heat losses. The MCDW signature was detected as a subsurface temperature maximum below this water layer at ~300 m. This feature was apparent at a number of locations in the Amundsen Sea (Walker et al., 2007; Wåhlin et al., 2010; Ha et al.,

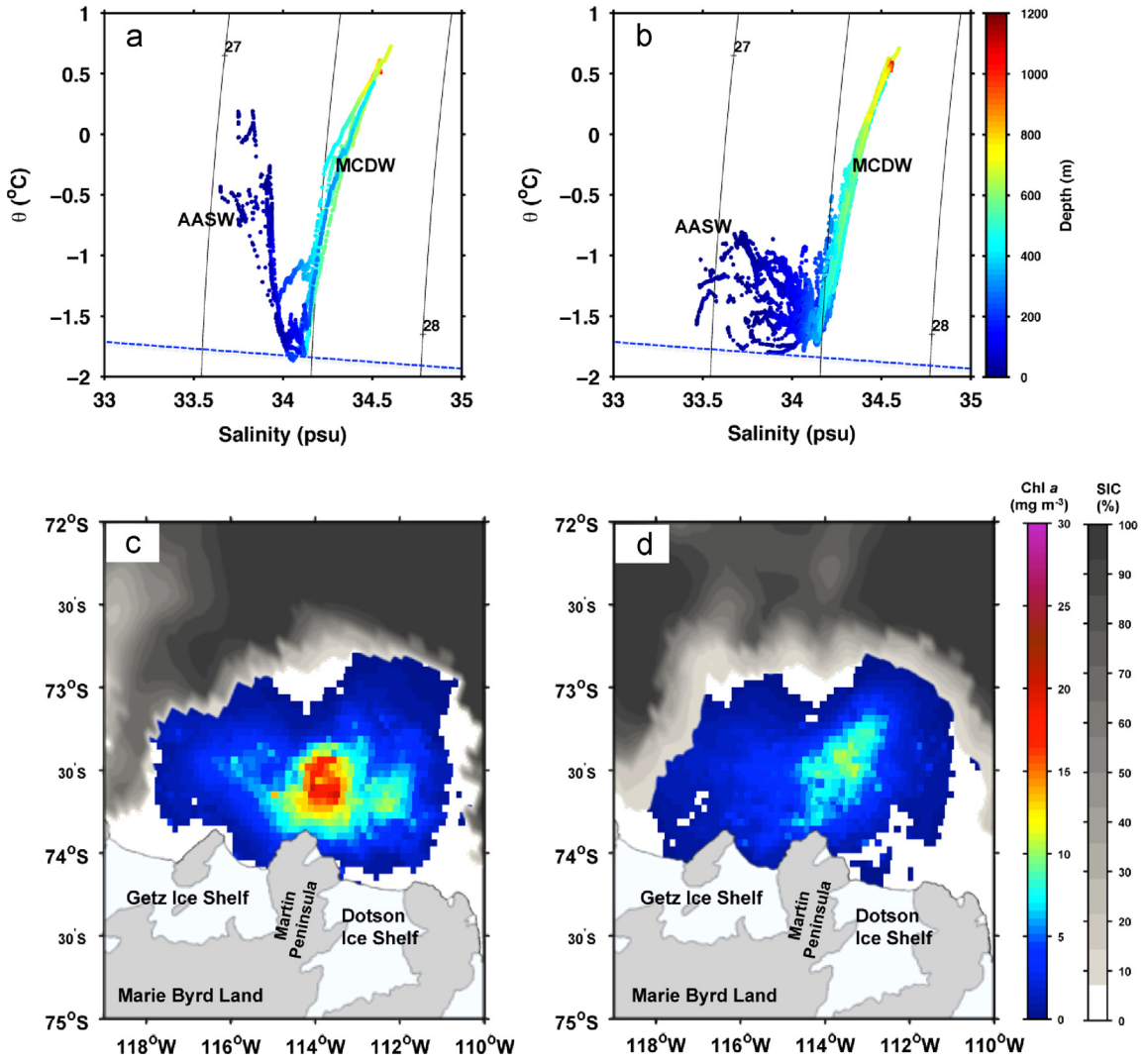

Fig. 2. Environmental conditions in the Amundsen Sea coastal polynya. Potential temperature (θ)-salinity (S) diagrams that correspond to AASW and MCDW in January 2011 (a) and February 2012 (b). The dashed line represents the freezing temperature. The Chl *a* and sea ice concentration were derived from MODIS Aqua data and SSM/I data, respectively, during the survey period of January 1 to 6 in 2011 (c) and of February 12 to 18 in 2012 (d).

2014). The salinity of AASW ranged from 33.6 to 34.2 psu in 2011 and from 33.4 to 34.2 psu in 2012, whereas the temperature ranged from −1.8 to 0.2 °C in 2011 and from −1.8 to −0.7 °C in 2012. Relatively cold AASW with low salinity was observed in 2012. The wide ranges in temperature and salinity values of the AASW indicate high spatial and temporal variability of this water mass that likely result from seasonal changes associated with melting and freezing of sea ice. In contrast the MCDW exhibited little seasonal variability.

The ice cover images highlight the spatial extent of the ASCP: the polynya widens along the Dotson and Getz ice shelves and spread northward to 73°S (Fig. 2(c) and (d)). The MODIS data indicate that there were elevated levels of phytoplankton biomass in the center of the ASCP in both 2011 and 2012 (Fig. 2(c) and (d)), although the levels were considerably greater in 2011 (>15 mg Chl a m^{-3}) compared with 2012 (<5 mg Chl a m^{-3}). The lowest level of phytoplankton biomass was observed around the edges of the polynya, particularly at the pack-ice boundary and ice-shelves.

Fig. 3 shows the seasonal variation of phytoplankton biomass for 2002–2012. Phytoplankton biomass begins to rapidly increase by November and the biggest increase occurs in December and January (Fig. 3). The phytoplankton bloom is generally observed in January and the bloom rapidly declines between January and February. The January 2011 survey took place at the peak of the phytoplankton bloom within the ASCP. In comparison, the February 2012 survey appears to have taken place later than the phytoplankton bloom. In general, a higher Chl *a* concentration was

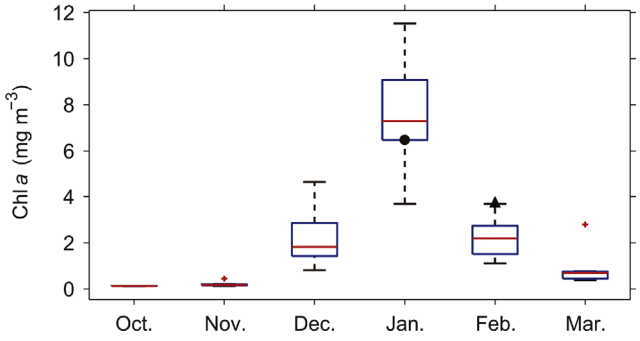

Fig. 3. Seasonal variations (October–March) of the mean phytoplankton biomass retrieved from the MODIS Aqua ocean color data with median (red line) and 25th and 75th percentile (blue box) for the years 2002–2012. The black dot and triangle indicate the survey period of the 2011 and 2012, respectively. (For interpretation of the references to color in this figure legend, the reader is referred to the web version of this article.)

observed during January 2011 (6.5 mg m^{-3}, compared with February 2012 (3.7 mg m^{-3}).

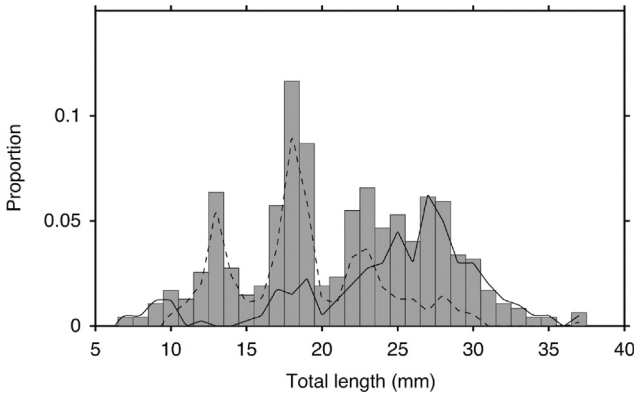

Fig. 4. Ice krill length-frequency distributions in the ASCP. Gray bars represent the length-frequency distribution in combined six data sets of the two surveys. The solid and dashed lines indicate the length-frequency distribution during January 2011 and February 2012, respectively.

3.2. Length frequency distribution of ice krill

Ice krill contributed more than 95% of the composition of all the Bongo net samples at five of the six stations sampled in 2011 and 2012; the exception was St. 11 in 2012, which exhibited a composition of 97% Antarctic krill (*Euphausia superba*). The mean length of Antarctic krill was 35.4 mm and varied from 20 to 55 mm. Ice krill was predominant in both years, and the total lengths ranged from 7 to 37 mm (Fig. 4) with a mean of 21.2 mm (SD=6.1 mm): in 2011 the mean was 24.5 mm (SD=6.2 mm, range of 7–37 mm) and in 2012 the mean was 18.7 mm (SD=4.8 mm, range of 10–37 mm).

3.3. Vertical distribution of scattering layers

The acoustic data obtained along six transects show the spatial and vertical pattern of the scattering layer in the ASCP (Fig. 5). The scattering layers with S_v values between −90 and −55 dB were observed mainly at depths from 20 to 250 m along each transect, and formed an almost constant horizontal layer. WMD of scattering layers was distributed at depths from 50 to 150 m and the most of WMD appeared to be deeper than the mixed layer (Schneider and

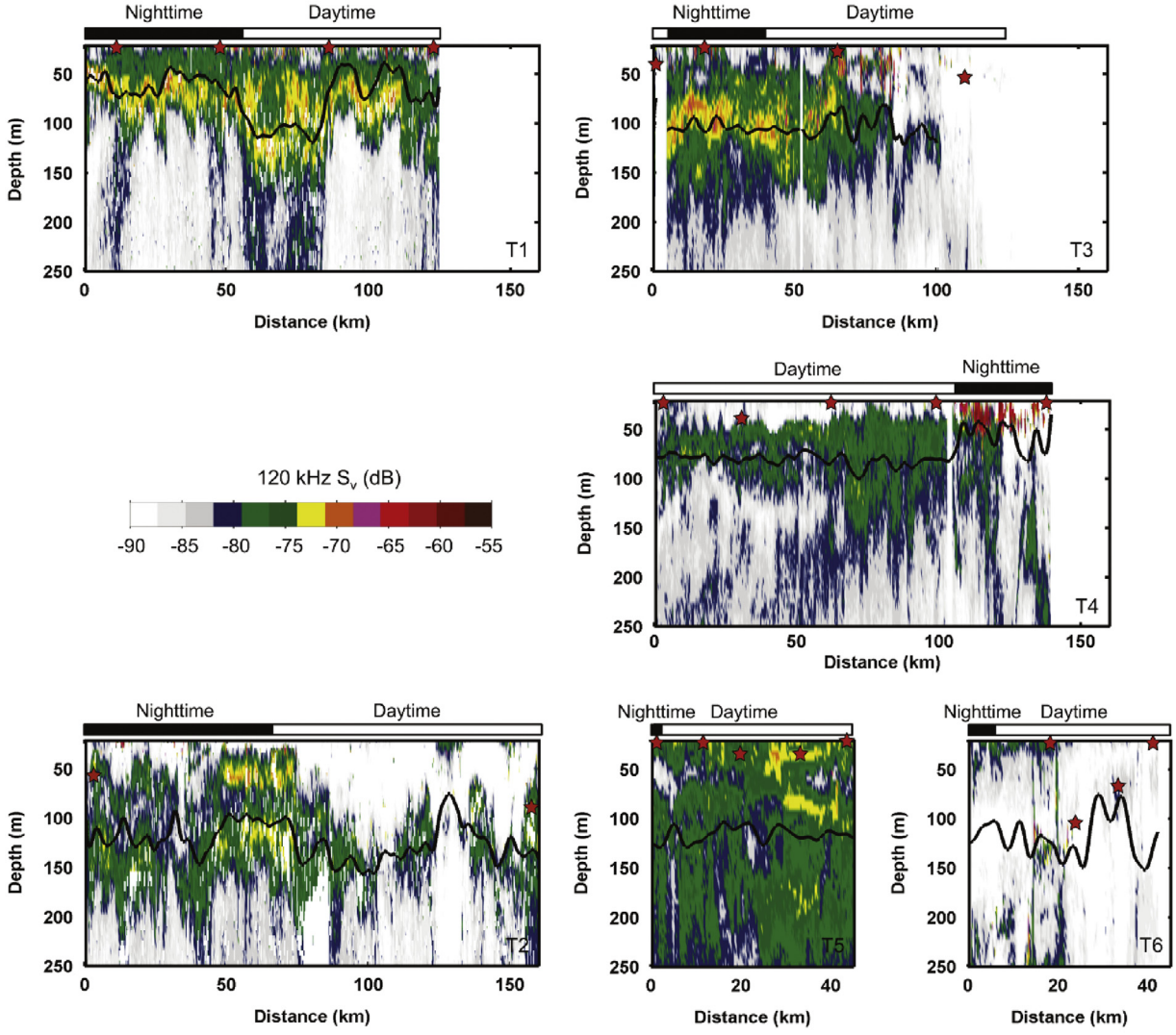

Fig. 5. Echograms for the top 250 m of the water column in the acoustic transect (T1–T6) at each stations. Red stars and solid black line denote the mixed layer depth and WMD of scattering layers, respectively.

Table 3
Mean volume backscattering strength (S_v, dB re 1 m^{-1}) of scattering layer in the Amundsen Sea coastal polynya.

Year	Transect name	Mean S_v (SD)		Mean WMD (SD)	
		Day	Night	Day	Night
2011	T1	−77.2 (33.8)	−79.2 (3.5)	80.0 (30.4)	60.7 (22.9)
	T2	−77.9 (2.1)	−80.8 (2.2)	128.8 (23.2)	116.4 (21.6)
2012	T3	−77.8 (3.4)	−78.7 (4.2)	106.1 (24.1)	103.9 (11.9)
	T4	−80.1 (2.1)	−81.5 (1.7)	74.4 (18.8)	78.9 (5.1)
	T5	−77.1 (1.4)	−76.8 (1.9)	115.12 (10.8)	128.8 (5.6)
	T6	−84.1 (2.9)	−81.8 (2.3)	120.3 (32.3)	119.1 (5.8)

The day data represent acoustic transects between 0000 and 1800 GMT.

Müller, 1990). The acoustic transects were undertaken during all periods of the day and night. Diel migration can influence the estimates of krill density (Demer and Hewitt, 1995; Everson, 1982), however, the mean S_v and WMD at each echogram did not show diel variation between day and night (Mann–Whitney *U*-test, $p < 0.05$, Table 3). Thus, given the lack of evidence of diel migration, we pooled the day and night data to estimate the ice krill density in the ASCP.

3.4. Identification of ice krill using acoustic data

The distribution of ice krill was estimated from the acoustic data, using a dual frequency identification window to identify acoustic targets as ice krill. The identification window can be tuned to identify krill of a certain size but is unable to determine between species of krill such as ice krill and Antarctic krill. The net data indicated that, apart from one station, ice krill was the dominant zooplankton and euphausiid species sampled. However, at St. 11, Antarctic krill comprised 97% of the net samples, which presented us with an opportunity to distinguish between the two species. Ice krill was observed in all transects with relatively high acoustic backscattering (S_v between −90 and −70 dB at 120 kHz) present in the top 200 m of the water column (Fig. 5). At St. 11, where Antarctic krill was caught, a second different target was observed in the acoustic data characterized by small patches of very high backscattering (greater than −70 dB at 120 kHz) existing only in the top 50 m (Fig. 6(a)). This type of target was only observed at St. 11. The examination of the signal strength at both 120 and 38 kHz (Fig. 6(b)) and the frequency response ($S_{v120-38}$) from the two targets (Fig. 6(c)) indicates that thresholds of −80 dB at 38 kHz and −65 dB at 120 kHz, as well as the $S_{v120-38}$ identification windows, can be used to distinguish ice krill from Antarctic krill in the acoustic data. Therefore, all ice krill densities presented in this paper are estimated from the acoustic data using both the upper threshold levels and the dB identification windows.

3.5. Ice krill density in the ASCP

Ice krill density estimated along each transect is shown in Fig. 7. The highest density of ice krill was 53 g wet mass m^{-2} observed along T3. The high mean density of ice krill (> 25 g wet mass m^{-2}) was observed at T3 and T5, and this value was approximately double the amount observed at other stations. The mean and median densities were similar for all transects (Fig. 7(a) and Table 4), which indicates that ice krill densities were evenly distributed over the whole range rather than skewed to high densities in small patches. The mean ice krill density was 15.9 g wet mass m^{-2} in 2011 (SD = 6.7), and 16.8 g wet mass m^{-2} in 2012 (SD = 12.7) for all acoustic transects combined.

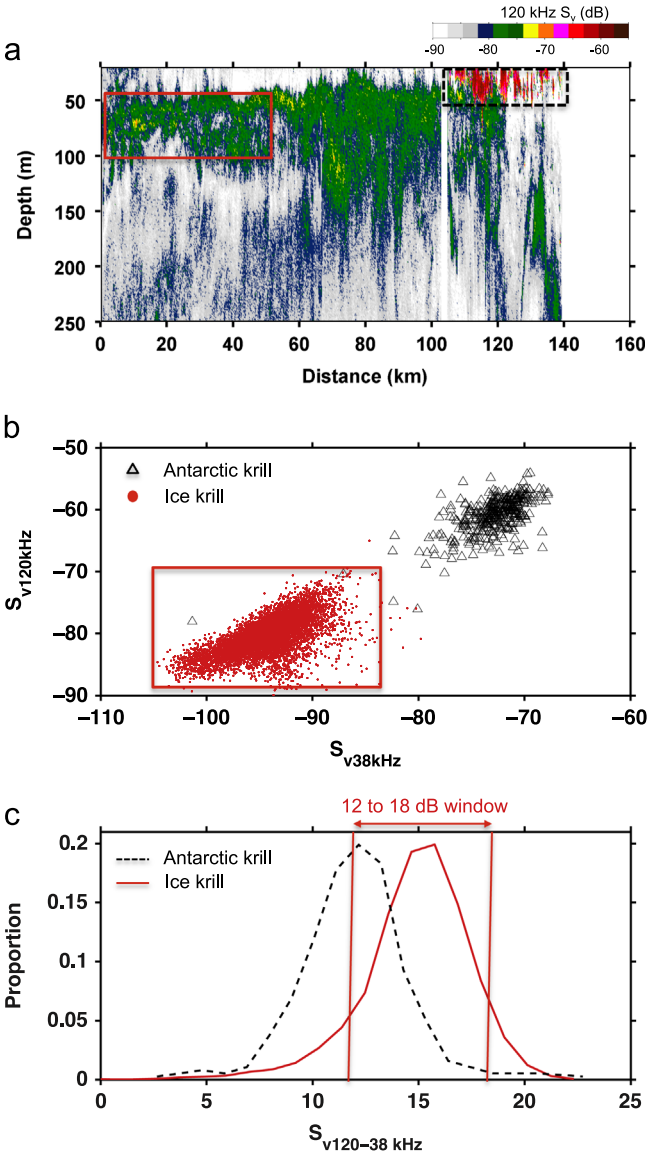

Fig. 6. Acoustic signals of Antarctic krill (box with dashed line) and ice krill (box with solid line) identified on a 120-kHz echogram in the acoustic transect (T4) during 2012 (a). Scatter plots of S_v at 120 and 38 kHz attributed to Antarctic krill (triangles) and ice krill (dots) (b). Differences in S_v attributed to Antarctic krill (solid line) and ice krill (dashed line) at 120 and 38 kHz (c). The 8 – 16 dB $S_{v120-38}$ window (Fig. 5(c)) and threshold technique with $S_{v120} < -70$ dB and $S_{v38} < -85$ dB (Fig. 5(b)) are applied to separate ice krill and Antarctic krill in the acoustic data.

Ice krill density exhibited a high degree of regional variability. In January 2011, the highest density (36 g m^{-2}) at T1 was observed in the center of the Dotson Trough over depths of 900 m. In T2 transect, the highest density of ice krill (35 g m^{-2}) was detected around the Martin Peninsula over depths of 400 m, whereas the density was low around the Dotson and Getz ice shelves. In February 2012, the highest density (53 g m^{-2}) of ice krill was observed between St. 3 and St. 5 along the T3 transect in water depths between 500 and 800 m. The density tended to decrease from the center of the Dotson Trough (St. 3) to shallower depths (St. 6), and the lowest density (less than 1 g m^{-2}) was observed near St. 6. In particular, there was an abrupt decline of densities between St. 5 and St. 6, which was located inside pack ice. In the center of the polynya (T4), the ice krill density was lower than those obtained in the other two transects and varied between

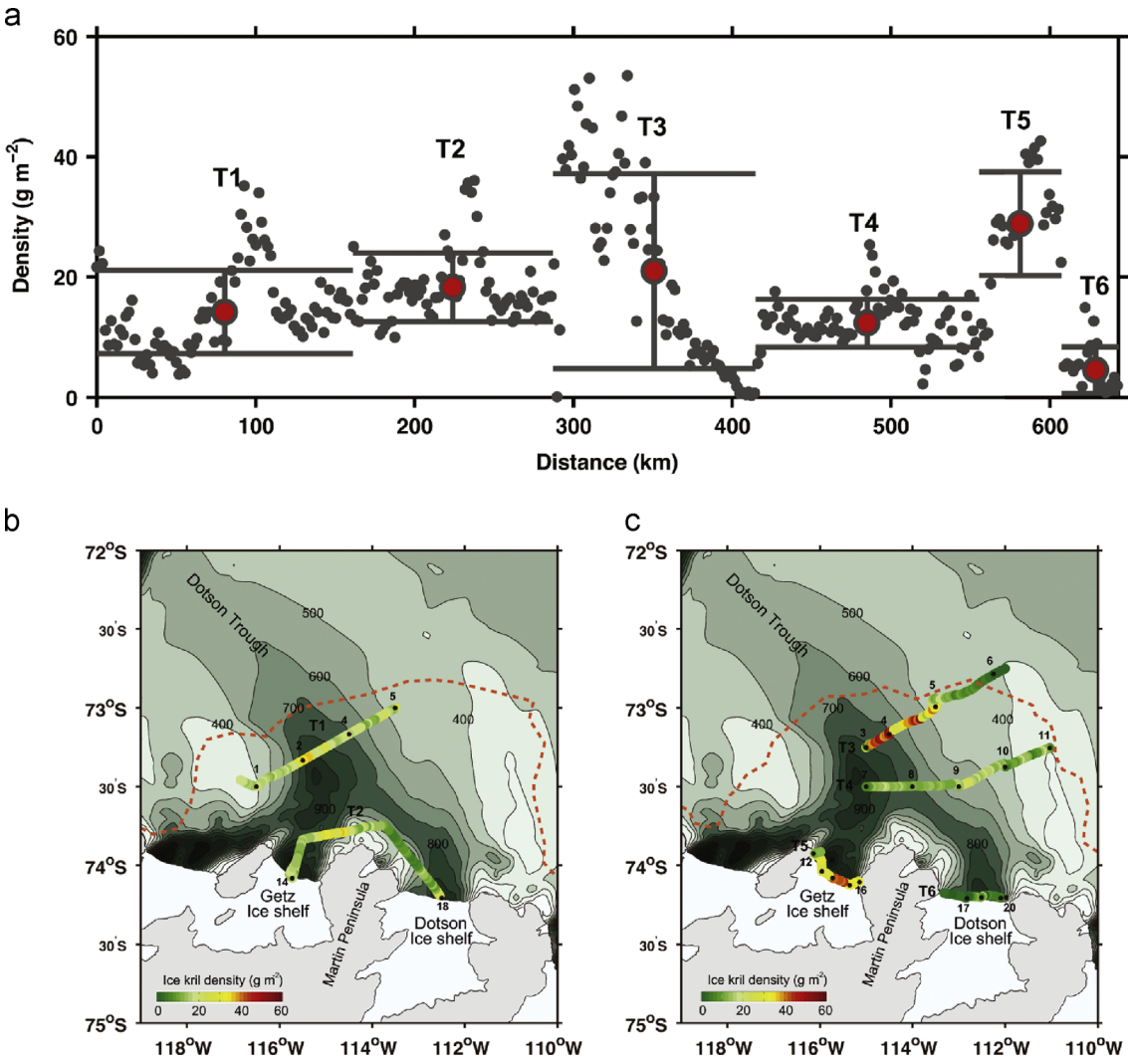

Fig. 7. Distribution of ice krill density within the ASCP, means (red circles with error bars) for acoustic transects (T1–T6) at each station (a). Distribution of the ice krill density on the bathymetry along the transects in 2011 (b) and 2012 (c). The dashed line is the pack ice boundary during the survey period. (For interpretation of the references to color in this figure legend, the reader is referred to the web version of this article.)

Table 4
Mean (standard deviation, SD) and median (standard error, SE) densities of ice krill (g m^{-2}) determined using the SDWBA target strength model. The transect densities were estimated from the 120-kHz S_v data using multi-frequency analysis methods.

Year	Transect name	Ice krill density (g m^{-2})	
		Mean (SD)	Median (SE)
2011	T1	18.3 (5.7)	16.8 (0.3)
	T2	14.2 (6.9)	13.1 (0.2)
2012	T3	30.0 (13.2)	28.1 (0.8)
	T4	12.3 (4.0)	12.0 (0.2)
	T5	28.9 (8.6)	28.6 (1.3)
	T6	4.5 (3.8)	3.3 (0.2)

Table 5
GLM results comparing ice krill density with environmental variables. Coefficients (z), error estimates (standard error, SE), and p value for the response of the ice krill density to the mean potential temperature (θ_m), the surface potential temperature (θ_s), the surface salinity (S_s), chlorophyll a (Chl a) and water depth (D). The θ_m and salinity (S_m) were depth-averaged from the surface to a depth of 250 m, whereas the θ_s and S_s were depth-averaged from the surface to a depth of 20 m. The Chl a was integrated from the surface to a depth of 100 m using the chlorophyll fluorescence data obtained from fluorometer mounted on the CTD frame. Log(Ice krill density)$=z+\theta_s+\theta_m$ S_s ($n=24$, $p<0.001$).

	Ice krill density ($n=24$)			
	Coefficient	SE	t	p
z	720.38	246.41	2.92	<0.05
θ_m	444.68	192.04	2.31	<0.05
θ_s	1.12	0.52	2.12	<0.05
S_s	−21.09	7.28	−2.89	<0.05
Chl a	−0.001	0.001	−1.26	0.22
D	−0.001	0.001	−0.66	0.51
θ_m: S_s	−13.08	5.67	−2.30	<0.05

2 and 25 g m^{-2}. The density near the center of the trough at the pack-ice boundary decreased in the direction of the Dotson ice shelf and the eastern trough in the Dotson Trough. In T4 around the Getz ice shelf, a high density was observed, which ranged between 10 and 43 g m^{-2}, whereas the density at T6 around the Dotson ice shelf was in the range of 1 to 15 g m^{-2}. The mean density of the Getz ice shelf was 29 g m^{-2}, which is six-fold higher than that of the Dotson ice shelf (5 g m^{-2}).

The association of ice krill density with environmental variables was investigated at each CTD station (2011 and 2012) using

a GLM analysis The mean temperature, the surface temperature, and the surface salinity were the most influential variables affecting the spatial variability of ice krill density in the ASCP (Table 5). In particular, the ice krill density showed significant strong positive relationships with the mean water temperature within the range of −1.8 to −0.9 °C (r^2=0.79). Ice krill densities were not significantly correlated with the indices of phytoplankton biomass such as integrated and surface Chl *a*, or water depth (Table 5).

4. Discussion

This study presents the first observation of the distribution of ice krill in the ASCP during the austral summer. We first discuss the caveats associated with our use of acoustic methods to quantify ice krill density and then investigate the distribution of ice krill within the ASCP and the factors that may promote its abundance in this system.

4.1. Uncertainties in assessing the distribution of ice krill

A central question to ecologists is whether a survey adequately represents the biological communities being investigated. The ice krill density estimates presented here were not obtained using a formal survey, instead they have been calculated along transects between point stations. As a result we have presented mean and standard deviation along these transects, rather than a biomass estimate for the area. Sampling krill is challenging, regardless of whether net- or acoustics-based methods are used (Atkinson et al., 2012). Net estimates are typically lower and frequently unrelated to acoustic estimates of density, suffering from issues of avoidance, differing catchability, heterogeneity of distribution and in particular low sampling volume (Kasatkina et al., 2004). Acoustically derived density estimates equally have a variety of uncertainties, in particular diel variability, species identification and acoustic dead zones.

In this study sampling was around the clock, so diel differences due to migration up to the surface out of range of the transducer is a potential problem (Demer and Hewitt, 1995). However, we observed only minor variations in S_v and the WMD between day and nights, indicating differences in density estimates were unlikely to be due to diel vertical migration. A second key area of uncertainty is calibration of the acoustic system, target identification and subsequent conversion to density. The 38-kHz acoustic system was only calibrated for the 2012 survey and calibration in ambient water type is recommended for each survey (Foote et al., 1987), however the environmental conditions were very similar during both years in this study and we are confident the 38 kHz transducer was performing correctly.

Our ability to distinguish between ice krill and Antarctic krill in the acoustic data was supported by net samples, which identified only one station (St. 11) containing significant numbers of species (Antarctic krill) other than ice krill. Here, we observed a distinctly different acoustic target (separated both on an upper acoustic threshold and dB difference method) that we attributed to adult Antarctic krill. Although juveniles and adults of the two species were encountered at St. 11 and were separable acoustically, it is possible that small juvenile Antarctic krill (of sizes overlapping those of ice krill) were encountered along the transect and misclassified as ice krill. This is a well-recognized problem in high-latitude acoustic studies (Amakasu et al., 2011), but given the overwhelming dominance of ice krill in the net samples, we have classified the density as ice krill.

The accuracy of a krill density estimate is closely proportional to the accuracy of the target strength (TS) when using acoustic scattering models. Application of the SDWBA requires particularly the orientation distribution and acoustic properties (the density contrast *g* and the speed of sound contrast *h*) of krill (Conti and Demer, 2006). Ice krill and Antarctic krill are biochemically different (Bottino, 1974; Kattner and Hagen, 1998, e.g., ice krill store wax esters while Antarctic krill store triacylglycerol and polar lipids) and their swimming orientations may differ, which could substantially alter their acoustic profiles (Chu et al., 2000; Chu and Wiebe, 2005). Chu and Wiebe (2005) showed that *h* is fairly similar between Antarctic and ice krill, whilst *g* is a little lower than Antarctic krill. This would decrease the TS predictions for ice krill, thereby resulting in a higher estimate of ice krill density. In this study, the acoustic properties of ice krill were considered to be similar to those of Antarctic krill, and parameterized for Antarctic krill (Demer and Conti, 2005) using the SDWBA. A further caveat is that we derived the density data using length-mass regressions for morphologically very similar Antarctic krill rather than for ice krill.

The estimated orientation distribution of ice krill was N[−8°, 9°] and N[13°, 19°] during 2011 and 2012, respectively. Considering that the SDWBA attributes the shape of the krill to a bent cylinder that this model is head up (+ orientations) or head down (− orientations), the maximum TS difference for 20 mm length krill ranging orientation from −8° to 13° with standard error of 15° is 0.78 dB for 120 kHz and 0.3 dB for 38 kHz. Thus, the effect of our estimated orientation distribution on the density is very small if one ignores the + or −.

Finally, our observations were limited to 20−250 m of water column due to the limitation of hull-mounted echo sounder. However large proportions of euphausiid population, including ice krill, can reside in the surface layer (Flores et al., 2011; Krakatistsa et al., 1993), and performs a pronounced diel vertical migration by visiting the depth in which the data cannot be achieved with a regular ship-based echo sounder (Siegel, 2005; Cisewski et al., 2010). A wide variety of krill species, including ice krill visit the seafloor to feed (Schmidt, 2010; Schmidt et al., 2011). However, our observations are from the summer where the availability of food in the productive surface waters should be high with a high number of ice krill most likely to be in those waters. Notwithstanding all of the above issues, we postulate that krill population density in the ASCP is high, and is dominated by ice krill.

4.2. Distribution of ice krill within the ASCP

The mean densities observed here are an order of magnitude higher than the only other acoustically-derived ice krill density estimate reported for the Antarctic continental shelf (Ross Sea, mean of 1.5 g m^{-2}, Azzali et al., 2006). Most other studies of ice krill density are based on net samples that give estimates two orders of magnitude lower than the ones observed here (Pakhomov and Perissinotto, 1996; Pakhomov et al., 1998; Guglielmo et al., 2009). Our values (15−17 g wet mass m^{-2}) are more comparable with acoustic estimates of Antarctic krill density at the Antarctic Peninsula, and approximately 50% of those from the Scotia Sea and South Georgia (Fielding et al., 2011). Although not an areal estimation the high densities observed here suggests ice krill are a potentially important, but poorly known contributor to these high-latitude shelf food webs.

The fact that the ASCP is one of the most productive polynyas may explain why we observed high ice krill densities. The ASCP seasonally averaged Chl *a* levels are 2.2 ± 3 mg m^{-3}, more than 40% higher than in the Ross Sea Polynya (Yager et al., 2012). Lee et al. (2013) found the abundance of ice krill to be positively correlated with Chl *a* concentration in the ASCP in 2010/2011 summer. However, a similar association was not observed in this study. Although satellite images show that the ASCP is productive

with large phytoplankton blooms, this bloom can be dominated by *Phaeocystis* spp. (Yang, unpublished data) and there is little evidence that it can be utilized by ice krill. It is more likely that the perennial pack ice boundary plays an important role in producing the high density of ice krill. The sea ice edge supports a nursery habitat for micro-zooplankton (Brierley and Thomas, 2002) and other metazoans (Daly and Macaulay, 1988; Marschall, 1988; Smith and Barber, 2007), ideal food for the omnivorous ice krill. This conclusion is supported by the observation that ice krill density decreased sharply in the seasonal pack ice zone (Fig. 6) and that krill density was significantly correlated with low temperature waters reflecting the recent contact with sea ice.

Antarctic krill were only observed at St. 11 during this study, within the seasonal pack ice zone. Previous studies have shown juvenile Antarctic krill are more abundant under pack ice than in open water in spring (Daly and Macaulay, 1988; Brierley et al. 2002). Occupying different positions within the polynya, the two krill species may not compete directly for the same food source in high Antarctic latitudes (O'Brien, 1987) and have different habitat preferences and biochemical composition (Bottino, 1974).

The ice krill density in 2012 was higher along the Getz ice shelf than the Dotson ice shelf. The two ice shelves seem to have different environmental conditions, with those near the Getz more favorable to ice krill. Rapid ice shelf melting has been linked to basal melting by warm water (Walker et al., 2007), and the different geological conditions of two ice shelves might cause different water column conditions around each ice shelf. Getz glacier water was warmer, less saline and had higher Chl *a* than Dotson glacier waters. This indicates a strong water column stratification, which might promote the higher ice krill density around the Getz ice shelf observed during both years.

In summary, we present a method for distinguishing ice krill and Antarctic krill with acoustic data, which was used to investigate the distribution of ice krill along acoustic transects in the ASCP. Ice krill are an important link between the sea ice, the water column and upper trophic levels, yet relatively little is known about their biomass and distribution, most likely linked to the challenges of sampling within sea ice. The acoustic discrimination method presented here could be the precursor to a biomass estimate being generated for the ASCP and other areas, if a suitable areal sampling strategy is employed.

The distribution of ice krill in this study was not well linked to Chl *a* distribution but to water mass properties (temperature and salinity). The diet of ice krill is thought to be carnivorous during early spring and become omnivorous at the onset of the spring phytoplankton bloom (Pakhomov et al., 1998). The timing of our observations here was after the onset of the spring bloom. It is possible, therefore, that our lack of observed relationship between krill and Chl *a* is because the phytoplankton bloom has switched from diatoms to *Phaeocystis* spp. and the krill have turned back to a more carnivorous diet. The trophic linkage between sea-ice algae, microzooplankton and ice krill needs to be further investigated.

Acknowledgments

The authors acknowledge the support and dedication of the captain and crews of *IBRV ARAON* for always completing the work with positive energy. We thank our field teams, which worked together under difficult conditions during the survey. The authors also thank the referees for their comments and suggestions, which improved several aspects of this paper. H. Dahms (Kaohsiung Medical University) and Y. Jiang provided helpful comments that helped improve the manuscript. D.B. Lee gave support to gather the net samples. This research was supported by KOPRI (PP14020), KIOST (PN65890), and the Inha University (INHA-49278) Research grants.

References

Amakasu, K., Ono, A., Hirano, D., Moteki, M., Ishimaru, T., 2011. Distribution and density of Antarctic krill (Euphausia superba) and ice krill (E. crystallorophias) off Adélie Land in austral summer 2008 estimated by acoustical methods. Polar Sci. 5 (2), 187–194.

Arrigo, K.R., van Dijken, G.L., 2003. Phytoplankton dynamics within 37 Antarctic Coastal Polynya systems. J. Geophys. Res. 108 (C8), 3271.

Arrigo, K.R., Lowry, K.E., van Dijken, G.L., 2012. Annual Changes in sea ice and phytoplankton in polynyas of the Amundsen Sea, Antarctica. Deep Sea Res. II 71, 5–15.

Atkinson, A., Nicol, S., Kawaguchi, S., Pakhomov, E., Quetin, L., Ross, R., Hill, S., Siegel, V., Tarling, G., 2012. Fitting *Euphausia superba* into southern ocean food-web models: a review of data sources and their limitations. CCAMLR Sci. 19, 219–245.

Azzali, M, Leonori, I., De Felice, A., Russo, A., 2006. Spatial-temporal relationships between two euphausiid species in the Ross Sea. Chem. Ecol. 22, 219–233.

Barber, D.G., Massom, R.A., 2007. The role of sea ice in Arctic and Antarctic polynyas. In: Smith Jr., W.O., Barber, D.G. (Eds.), Polynyas: Windows to the world. Elsevier, Amsterdam.

Bottino, N.R., 1974. The fatty acids of Antarctic phytoplankton and euphausiids. Fatty acid exchange among trophic levels of the Ross Sea. Mar. Biol. 27, 197–204.

Brierley, A.S., Fernandes, P.G., Brandon, M.A., Armstrong, F., Millard, N.W., McPhail, S.D., Stevenson, P., Pebody, M., Perrett, J., Squires, M., Bone, D.G., Griffiths, G., 2002. Antarctic krill under sea ice: elevated abundance in a narrow band just south of Ice Edge. Science 295, 1890–1892.

Brierley, A.S., Thomas, D.N., 2002. Ecology of Southern Ocean pack ice. Adv. Mar. Biol. 43, 171–276.

Bushuev, S.G., 1986. Feeding of Minke whales, *Balaenoptera acutorostrata*, in the Antarctic. Rep. Int. Whal. Comm. 36, 241–245.

CCAMLR, 2010. Report of the Fifth Meeting of the Subgroup on Acoustic Survey and Analysis methods. SC-CCAMLR-XXIX/6.

Cisewski, B., Strass, V.H., Rhein, M., Kragefsky, S., 2010. Seasonal variation of diel vertical migration of zooplankton backscatter time series data in the Lazarev Sea, Antarctica. Deep Sea Res. I 57, 78–94.

Conti, S.G., Demer, D.A., 2006. Improved parameterization of the SDWBA for estimating krill target strength. ICES J. Mar. Sci. 63, 928–935.

Chu, D., Wiebe, P.H., Copley, N., 2000. Inference of material properties of zooplankton from acoustic and resistivity measurements. ICES J. Mar. Sci. 57, 1128–1142.

Chu, D., Wiebe, P.H., 2005. Measurements of sound-speed and density contrasts of zooplankton in Antarctic waters. ICES J. Mar. Sci. 62, 818–831.

Daly, K.L., Macaulay, M.C., 1988. Abundance and distribution of krill in the ice edge zone of the Weddell Sea, austral spring 1983. Deep Sea Res. I 35, 21–41.

Madureira, L.S.P., Everson, I., Murphy, E.J., 1993. Interpretation of acoustic data at two frequencies to discriminate between Antarctic krill (*Euphausia superba* Dana) and other scatterers. J. Plankton Res. 15, 787–802.

Marschall, H.P., 1988. The overwintering strategy of antarctic krill under the pack-ice of the Weddell Sea. Polar Biol. 9, 129–135.

Demer, D.A., Hewitt, R.P., 1995. Bias in acoustic density estimates of *Euphausia superba* due to diel vertical migration. Deep Sea Res. I 42, 455–475.

Demer, D.A., Conti, S.G., 2005. New target-strength model indicates more krill in the Southern Ocean. ICES J. Mar. Sci. 62, 25–32.

Everson, I., 1982. Diurnal variations in mean volume-backscattering strength of an Antarctic krill (*Euphausia superba*) patch. J. Plankton Res. 4, 155–162.

Everson, I., 1987. Some aspects of the small scale distribution of *Euphausia crystalorophias*. Polar Biol. 8, 9–15.

Fielding, S., Watkins, J.L., Cossio, A., Reiss, C., Watters, G., Calise, L., Skaret, G., et al. 2011. The ASAM 2010 assessment of krill biomass for area 48 from the Scotia Sea CCAMLR 2000 synoptic survey. CCAMLR Document WG-EMM 11/20, CCAMLR, Hobart, Australia.

Flores, H., van Franeker, J.A., Cisewski, B., Leach, H., Van de Putte, A.P., Meesters, E.H.W.G., Bathmann, U., Wolff, W.J., 2011. Macrofauna under sea ice and in the open surface layer of the Lazarev Sea, Southern Ocean. Deep Sea Res. II 58, 1948–1961.

Foote, K.G., Knudsen, H.P., Vestnes, G., MacLennan, D.N., Simmonds, E.J., 1987. Calibration of acoustic instruments for fish density estimation: A practical guide. ICES Co-operative Research Report, vol. 144; p. 69.

Foote, K.G., 1990. Speed of sound in *Euphausia superba*. J. Acoust. Soc. Am. 87 (4), 1405–1408.

Guglielmo, L., Donato, P., Zagami, G., Granata, A., 2009. Spatial-temporal distribution and abundance of *Euphausia crystallorophias* in Terra Nova Bay (Ross Sea, Antarctica) during austral summer. Polar Biol. 32, 347–367.

Ha, H.K., Wåhlin, A.K., Kim, T.W., Lee, S.H., Lee, J.H., Lee, H.J., Hong, C.S., Arneborg, L., Björk, G., Kalén, O., 2014. Circulation and modification of warm deep water on the central Amundsen Shelf. J. Phys. Oceanogr , http://dx.doi.org/10.1175/JPO-D-13-0240.1.

Hamner, W.M., Hamner, P.P., Strand, S.W., Gilmer, R.W., 1983. Behavior of Antarctic krill, *Euphausia superba*: chemoreception, feeding, schooling, and moulting. Science 220, 433–435.

Holt, E.W.L., Tattersall, W.M., 1906. Preliminary notice of the Schizopoda collected by HMS 'Discovery' in the Antarctic Region. Ann. Mag. Nat. Hist. 17 (97), 1–11.

Hosie, G.W., Cochran, T.G., 1994. Mesoscale distribution patterns of macrozooplankton communities in Prydz Bay, Antarctica January to February 1991. Mar. Ecol. Prog. Ser. 106, 21–39.

Hubold, G., 1985. The early life-history of the high-Antarctic silverfish *Pleuragramma antarcticum*. In: Siegfried, W.R., Condy, P.R., Laws, R.M. (Eds.), Antarctic Nutrient Cycles and Food Webs. Springer, Berlin, pp. 445–451.

Kasatkina, S.M., Goss, C., Emery, J.H., Takao, Y., Litvinov, F.F., Malyshko, A.P., Shnar, V.N., Berezhinsky, O.A., 2004. A comparison of net and acoustic estimates of krill density in the Scotia Sea during the CCAMLR 2000 Survey. Deep Sea Res. II 57, 1289–1300.

Kattner, G., Hagen, W., 1998. Lipid metabolism of the Antarctic euphausiid *Euphausia crystallorophias* and its ecological implications. Mar. Ecol. Prog. Ser. 170, 203–213.

Kittel, W., Ligowski, R., 1980. Algae found in the food of *E. crystallorophias*. Pol. Polar Res. 1, 129–137.

Lee, D.B., Choi, K.H., Ha, K.H., Yang, E.J., Lee, S.H., Lee, SH, Shin, H.C., 2013. Mesozooplankton distribution patterns and grazing impacts of copepods and *Euphausia crystallorophias* in the Amundsen Sea, West Antarctica, during austral summer. Polar Biol. , http://dx.doi.org/10.1007/s00300-013-1314-8.

McClain, C.R., Cleave, M.L., Feldman, G.C., Gregg, W.W., Hooker, S.B., Kuring, N., 1998. Science quality SeaWiFS data for global biosphere research. Sea Technol. 39, 10–16.

McGehee, D.E., O'Driscoll, R.L., Traykovski, M., 1998. Effects of orientation on acoustic scattering from Antarctic krill at 120 kHz. Deep Sea Res.I 45, 1273–1294.

Melnikov, I.A., Spiridinov, V.A., 1996. Antarctic krill under perennial sea ice in the western Weddel Sea. Antarct. Sci. 8, 323–329.

Morris, D.J., Watkins, J.L., Ricketts, C., Buchholz, F., Priddle, J., 1988. An assessment of the merits of length and weight measurements of Antarctic krill *Euphausia superba*. Brit. Antarct. Surv. B. 79, 27–50.

Myriax. 2012. Help file 5.20 for Echoview [Internet]. Myriax, Hobart, TAS, AU, Accessed 6 Apr 2011, ⟨http://support.echoview.com/WebHelp/Echoview.htm⟩.

Pakhomov, E.A., Perissinotto, R., 1996. Antarctic neritic krill Euphausia crystallorophias: spatio-temporal distribution, growth and grazing rates. Deep Sea Res. Part I 43, 59–87.

Pakhomov, E.A., Perissinotto, R., Froneman, P.W., 1998. Abundance and tropho dynamics of *Euphausia crystallorophias* in the shelf region of the Lazarev Sea during austral spring and summer. J. Mar. Syst. 17, 313–324.

Roe, H.S.J., Angel, M.V., Badcock, J., Domanski, P., James, P., Pugh, P.R., Thurston, M.H., 1984. The diel migrations and distributions within a mesopelagic community in the North East Atlantic. 1. Introduction and sampling procedures. Prog. Oceanogr. 13, 245–260.

Sala, A., Azzali, M., Russo, A., 2002. Krill of the Ross Sea: distribution, abundance and demography of *Euphausia superba* and *Euphausia crystallorophias* during the Italian Antarctic Expedition (January-February 2000). Sci. Mar. 66 (2), 123–133.

Schmidt, K., 2010. Food and feeding in Northern krill (*Meganyctiphanes norvegica* SARS). Adv. Mar. Biol. 57, 127–171. http://dx.doi.org/10.1016/B978-0-12-381308-4.00005-4.

Schmidt, K., Atkinson, A., Steigenberger, S., Fielding, S., et al., 2011. Seabed foraging by Antarctic krill: implications for stock assessment, bentho-pelagic coupling, and the vertical transfer of iron. Limnol. Oceanogr. 56, 1411–1428.

Schneider, N., Müller, P., 1990. The meridional and seasonal structures of the mixed-layer depth and its diurnal amplitude observed during the Hawaii-to-Tahiti Shuttle experiment. J. Phys. Oceanogr. 20, 1395–1404.

Siegel, V., Piatkowski, U., 1990. Variability in the macrozooplankton community off the Antarctic Peninsula. Polar Biol. 10, 373–386.

Siegel, V., 2005. Distribution and population dynamics of *Euphausia superba*: summary of recent findings. Polar Biol. 29, 1–22.

Smith Jr., W.O., Barber, D.G., 2007. Polynyas: Windows to the world. Elsevier, Amsterdam.

Thomas, P.G., Green, K., 1988. Distribution of *Euphausia crystallorophias* within Prydz Bay and its importance to the inshore marine ecosystem. Polar Biol. 8, 327–331.

Walker, D.P., Brandon, M.A., Jenkins, A., Allen, J.T., Dowdeswell, J.A., Evans, J., 2007. Oceanic heat transport onto the Amundsen Sea shelf through a submarine glacial trough. Geophys. Res. Lett. 34 (L02602), http://dx.doi.org/10.1029/2006GL028154.

Wåhlin, A.K., Yuan, X., Bjork, G., Nohr, C., 2010. Inflow of warm circumpolar deep water in the central Amundsen shelf. J. Phys. Oceanogr. 40 (6), 1427–1434.

Wåhlin, A.K., Kalén, O., Arneborg, L., Björk, G., Carvajal, G., Ha, H.K., Kim, T.W., Lee, S.H., Lee, J.H., Stranne, C., 2013. Variability of warm deep water inflow in a submarine trough on the Amundsen Sea Shelf. J. Phys. Oceanogr. 43, 2054–2070.

Watkins, J.L., Brierley, A.S., 1996. A post-processing technique to remove background noise from echo integration data. ICES J. Mar. Sci. 53, 339–344.

Whitehead, M.D., Johnstone, G.W., Burton, H.R., 1990. Annual fluctuations in productivity and breeding success of Adelie penguins and fulmarine petrels in Prydz Bay, East Antarctica. In: Kerry, KR, Hempel, G. (Eds.), Antarctic ecosystems. Ecological change and conservation. Springer, Berlin, pp. 214–223.

Yager, P.L., Sherrell, L.M., Stammerjohn, S.E., Alderkamp, A.C., Schofield, O., Abrahamsen, E.P., Arrigo, K.R., Bertilsson, S., Garay, D.L., Guerrero, R., Lowry, K.E., Moksnes, P.-O., Ndungu, K., Post, A.F., Randall-Goodwin, E., Riemann, L., Severmann, S., Thatje, S., van Dijken, G.L., Wilson, S., 2012. ASPIRE: The Amundsen Sea Polynya International Research Expedition. Oceanography 25 (3), 40–53.